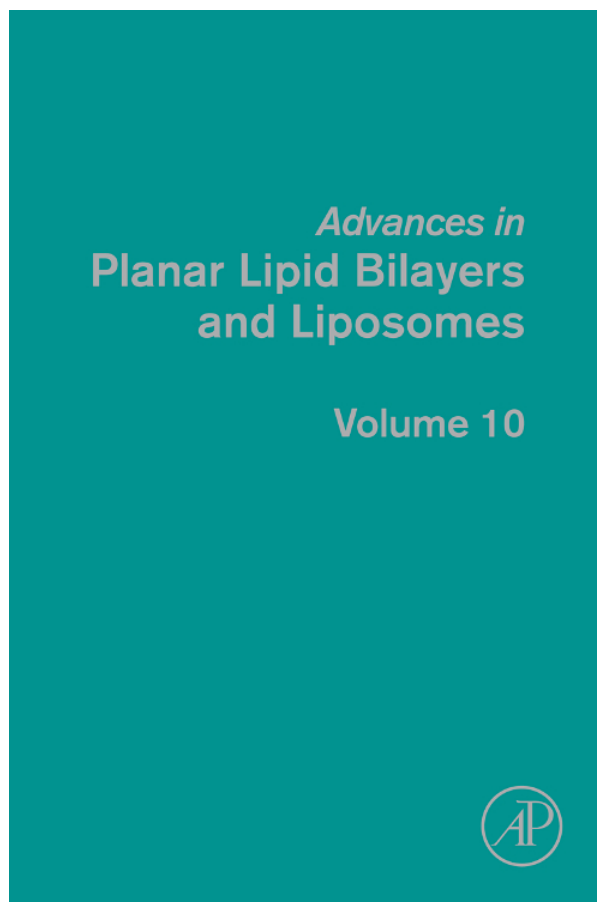


**Provided for non-commercial research and educational use only.  
Not for reproduction, distribution or commercial use.**

This chapter was originally published in the book *Advances in Planar Lipid Bilayers and Liposomes*, Vol. 10, published by Elsevier, and the attached copy is provided by Elsevier for the author's benefit and for the benefit of the author's institution, for non-commercial research and educational use including without limitation use in instruction at your institution, sending it to specific colleagues who know you, and providing a copy to your institution's administrator.



All other uses, reproduction and distribution, including without limitation commercial reprints, selling or licensing copies or access, or posting on open internet sites, your personal or institution's website or repository, are prohibited. For exceptions, permission may be sought for such use through Elsevier's permissions site at:

<http://www.elsevier.com/locate/permissionusematerial>

From: Maruša Lokar, Šárka Perutková, Veronika Kralj-Iglič, Aleš Iglič, and Peter Veranič, Membrane Nanotubes in Urothelial Cell Line T24. In A. Leitmannova Liu and Aleš Iglič, editors: *Advances in Planar Lipid Bilayers and Liposomes*, Vol. 10, Burlington: Academic Press, 2009, pp. 65-94.  
ISBN: 978-0-12-374823-2  
© Copyright 2009 Elsevier Inc.  
Academic Press.

## MEMBRANE NANOTUBES IN UROTHELIAL CELL LINE T24

Maruša Lokar,<sup>1,\*</sup> Šárka Perutková,<sup>1</sup> Veronika Kralj-Iglič,<sup>2</sup>  
Aleš Iglič,<sup>1</sup> and Peter Veranič<sup>3</sup>

### Contents

1. Introduction	66
2. T24 Cell Line and Membrane Nanotubes	72
2.1. Types of Membrane Nanotubes, Their Structural and Functional Properties	72
2.2. Vesicular Dilatations on Membrane Nanotubes	78
3. Formation and Stability of Type I Membrane Nanotubes	82
3.1. On the Role of Small Anisotropic Protein–Lipid Nanodomains in Formation and Stabilization of Membrane Nanotubes	85
4. Concluding Remarks	91
References	91

### Abstract

Membrane nanotubes (also referred as tunnelling nanotubes—TNTs, nanotubes, cytonemes), that directly connect separated neighboring cells, may offer a very specific and effective way of intercellular transport and communication. Our experiments on T24 cell line show that TNTs can be divided into two types with respect to their biochemical and biophysical characteristics and the nature of their formation. As type I were characterized the nanotubes which are shorter, more dynamic and contain actin filaments. These structures remain stable even if underlying actin cytoskeleton is disintegrated by cytochalasin D. The nanotubes of type II are much longer, appear more stable and contain cytokeratin filaments. In both types microtubules can be found, but this type of cytoskeleton is present in only a small fraction of the TNTs. On the nanotubes of

\* Corresponding author. Tel.: + 386 1 4768 235;  
E-mail address: [marusa.lokar@fe.uni-lj.si](mailto:marusa.lokar@fe.uni-lj.si)

<sup>1</sup> Laboratory of Biophysics, Faculty of Electrical Engineering, University of Ljubljana, Tržaška 25, SI-1000 Ljubljana, Slovenia

<sup>2</sup> Laboratory of Clinical Biophysics, Institute of Biophysics, Faculty of Medicine, University of Ljubljana, Vrazov trg 2, SI-1000 Ljubljana, Slovenia

<sup>3</sup> Institute of Cell Biology, Faculty of Medicine, University of Ljubljana, Lipičeva 2, SI-1000 Ljubljana, Slovenia

both types small vesicular dilatations were found as an integral part of the nanotubes (i.e., dilatations of the nanotubes, gondolas). Vesicular dilatations of type I nanotubes move along the nanotubes in both directions, while the vesicular dilatations of type II nanotubes do not move along the nanotubes. Both TNTs by themselves and the transporting gondolas were proposed to be involved in intercellular communication and transport. The possible mechanisms of stabilization of membrane nanotubular protrusions and TNTs are also discussed.

## ABBREVIATIONS

CMFDA	5-Chloromethylfluorescein diacetate
DiD	1,1'-Dioctadecyl-3,3,3,3'-tetramethylindodicarbocyanine
DiI	1,1'-Dioctadecyl-3,3,3,3'-tetramethylindodicarbocyanine
DiO	3,3'-Dilinoleyloxycarbocyanine
EFGP	Enhanced green fluorescent protein
FITC	Fluorescein isothiocyanate
GFP	Green fluorescent protein
GPI	Glycosyl-phosphatidylinositol
HLA, -B, -C	Human leukocyte class I antigens
TNTs	Tunneling nanotubes
TRITC	Tetramethylrhodamine isothiocyanate

## 1. INTRODUCTION

Cell-to-cell communication is one of the fundamental processes in the development and homeostasis of multicellular organisms. For this purpose organisms have evolved diverse mechanisms to communicate on the level of connected or/and spatially separated cells. The most common mechanisms depend on secretion of diffusible signal molecules (like hormones, growth factors) that bind to specific receptors in/on target cells [1]. A few years ago a novel type of cell-to-cell connection was discovered, where two spatially separated cells are connected by a long, thin tubular membranous structures [43]. They were named tunnelling nanotubes (TNTs) and are now known as membrane nanotubes. The membrane nanotubes were found in cultures and cocultures of both permanent cell lines and primary cultures (see [Tables 1 and 2](#)), mostly between cells that are weakly connected to each

**Table 1** Human and animal cell lines shown to form TNTs and their characteristics

Cell lines forming TNTs		Morphology			Transferred cellular components (markers)		
(From)	$\Phi$ (diameter) l (length)	Prevalence; form	Cytosolic continuity	Junction <sup>a</sup>	Cytoskeleton (filament binding proteins)	Cytoplasmic components (dyes)	Membrane components (dyes)
Rat pheochromocytoma cells (PC12) [43]	$\Phi = 50\text{--}200\text{ nm}$ $l = 16\text{--}60\ \mu\text{m}$	Few; straight, rarely branched, above substratum	ND	Yes	F-actin (myosin Va)	EGFP-actin	f-EGFP
Human embryonic kidney cells (Hek-293) [15]	ND	Few	ND	ND	F-actin (myosin Va)	ND	(DiI, DiO, DiD)
Normal rat kidney cells (NRK) [15]	ND	Many; form ND	ND	ND	ND	Endocytic organelles (DiD)	(DiI, DiO, DiD)
Primary human T-cells [48]	$\Phi = 180\text{--}380\text{ nm}^a$ $l = 30\text{--}50\ \mu\text{m}$ , some $\leq 200\ \mu\text{m}$	Many; straight, curved in 3D environment, rarely branched, above substratum	No <sup>b</sup>	Yes	F-actin	ND	ND
Jurkat T-cells [48]	$\Phi = \text{ND}$ $l = \sim 22\ \mu\text{m}$ , some $\leq 100\ \mu\text{m}$ in a 3D mimic of ECM	Many; straight, curved in 3D environment, rarely branched, above substratum	No <sup>b</sup>	Yes	F-actin	GFP, (CFDA, calcein)	GFP-I-CAM1, GFP-HLA-Cw7, GPI-GFP (DiO, DiD), HIV-1 Gag-GFP

(continued)

**Table 1** (continued)

Cell lines forming TNTs		Morphology			Transferred cellular components (markers)		
(From)	$\Phi$ (diameter) l (length)	Prevalence; form	Cytosolic continuity	Junction <sup>a</sup>	Cytoskeleton (filament binding proteins)	Cytoplasmic components (dyes)	Membrane components (dyes)
EBV-transformed human B cell line (721.221) [41]	ND	ND	ND	ND	ND	ND	GPI-GFP, HLA-Cw6 in coculture with human peripheral blood NK cells
Transitional cell carcinoma of urinary bladder cells (T24) [51]	$\Phi = 60\text{--}200\text{ nm}$ l = most < 30 $\mu\text{m}$ , some $\leq 120\text{ }\mu\text{m}$	Many: multiple, straight, on the substratum, rare above substratum	Yes <sup>b</sup>	Yes	Only F-actin cytokeratin 7, F-actin + microtubules ( $\alpha$ -tubulin)	Actin-GFP, (CMFDA)	Choleratoxin-GFP (DiI, DiO)
Transitional cell papilloma of urinary bladder cells (RT4) (Lokar <i>et al.</i> , unpublished)	ND	Few, on the substratum	ND	ND	F-actin	ND	ND
DU 145 human prostate cancer cells [52]	$\Phi$ : thinner 100–200 nm, thicker ( $\geq 1\text{ }\mu\text{m}$ ) l = few $\mu\text{m}$ – 100 $\mu\text{m}$		Yes	ND	Microtubules	Mitochondria (MitoTracker) lysosomes	ND
Human glioblastoma cells (U-87 MG) [42]	$\Phi = 42\text{--}54\text{ nm}$ l = tens of $\mu\text{m}$	Straight	ND	ND	F-actin	Vesicle trafficking under stress conditions	ND

THP-1 monocytes [40]	$\Phi = \sim 35\text{--}250\text{ nm}$ $l = <100\ \mu\text{m}$	Many	Yes <sup>b</sup>	ND	F-actin	Ca <sup>2+</sup> (Lucifer Yellow)	HLA-A,B, C class I MHC
Human hepatic cells (Hep G2) [54]	ND	Few	ND	ND	ND	ND	ND
Dendritic cells from peripheral blood monocytes [53]	$\Phi = \sim 35\text{--}250\text{ nm}$ $l = <100\ \mu\text{m}$	Many	Yes <sup>b</sup>	ND	ND	Ca <sup>2+</sup> (Lucifer Yellow)	HLA-A,B, C class I MHC
Human monocyte-derived macrophages [40, 41]	thin ( $<0.7\ \mu\text{m}$ ) thick ( $>0.7\ \mu\text{m}$ )	Many: thick prevalent, most are connecting apical parts of the cells, some are branched	ND	No	F-actin, F-actin + microtubules	Endosomes (DiD) mitochondria $\Phi =$ (Mito Tracker) lysosomes (LysoTracker), EB1-GFP	ND
Primary rat astrocytes [17]	$\Phi = \sim 100\text{ nm}$ $l = \text{several}\ \mu\text{m}$ $l = <1\ \mu\text{m}$ $l = >100\ \mu\text{m}$	Many, branched	ND	ND	F-actin	ND	ND
Hematopoietic stem and progenitor cells [14]		No data				No data	
Bovine mammary gland epithelial cells (BMGE) [54]		No data				No data	
Primary cultures of mouse medulla [15]		No data				No data	
Murine macrophage J477 cells [40]		No data				No data	

ND — not determined.

<sup>a</sup> Was assessed by transmission electron microscopy.

<sup>b</sup> Was proved indirectly by measuring calcium fluxes.

**Table 2** Cocultures of cell lines shown to form TNTs between different cell types

Coculture (from)	Transferred cellular component (dye)
PC12 and NRK cells [15]	Endosome related cell organelle (DiI, DiO, DiD)
PC12 and Hek-293 cells [15]	Endosome related cell organelle (DiI, DiO, DiD)
Hek-293 and NRK cells [15]	Endosome related cell organelle (DiI, DiO, DiD)
722.221 and NK cells cells [40]	Surface receptor HLA-Cw6-GFP
macrophages and NK cells [40]	ND, seen upon separation
Neonatal rat cardiomyocytes and adult human endothelial progenitor (EPC) cells [29]	Mitochondria (MytoTracker), GFP
Dendritic and THP-1 cells [40]	Ca <sup>2+</sup>

other or in those which are actively migrating and seeking for bacteria or attachment to neighboring eukaryotic cells. Nanotubes exist also in cells with limited ability of movement and strong intercellular connections like epithelial cells. The diameter of these membrane nanostructures ranges from 30 to 400 nm, in some cases up to 1  $\mu\text{m}$ , and their length can span for more cell diameters, depending on the cell type. They are versatile in ultrastructure and formation, and consequently also in function (reviewed by Refs. [9, 15]). Although TNTs are versatile, they share some common features like the presence of cytoskeleton and cytoskeleton-associated proteins. Through them different cellular material is being transported—from signaling molecules, soluble cytoplasmic proteins, membrane proteins and cell organelles [15, 16, 20, 21, 43, 51], to viruses [46, 47, 49] and bacteria. Viruses and bacteria are being transported only upon nanotube surfaces [41].

There is a considerable heterogeneity present between membrane nanotubes. They differ in their cytoskeletal composition, diameter, length, proposed function, ability to form cytoplasmic continuity. Ongoing studies of relatively young field in different cellular models are focused primarily on morphology, transported material and their frequency, but little is known about their biophysical properties, what factors influence their formation, what is the driving force of their formation, which protein complexes are involved in their dynamics and initiation of cell-to-cell contacts.

Considering their heterogeneity it is not an easy task to subdivide them ubiquitously into distinct types, since membrane nanotubes differ much from one cell type to another and their properties sometimes overlap between designated forms. Our classification of membrane nanotubes, in accordance with other authors, is presented in Fig. 1.

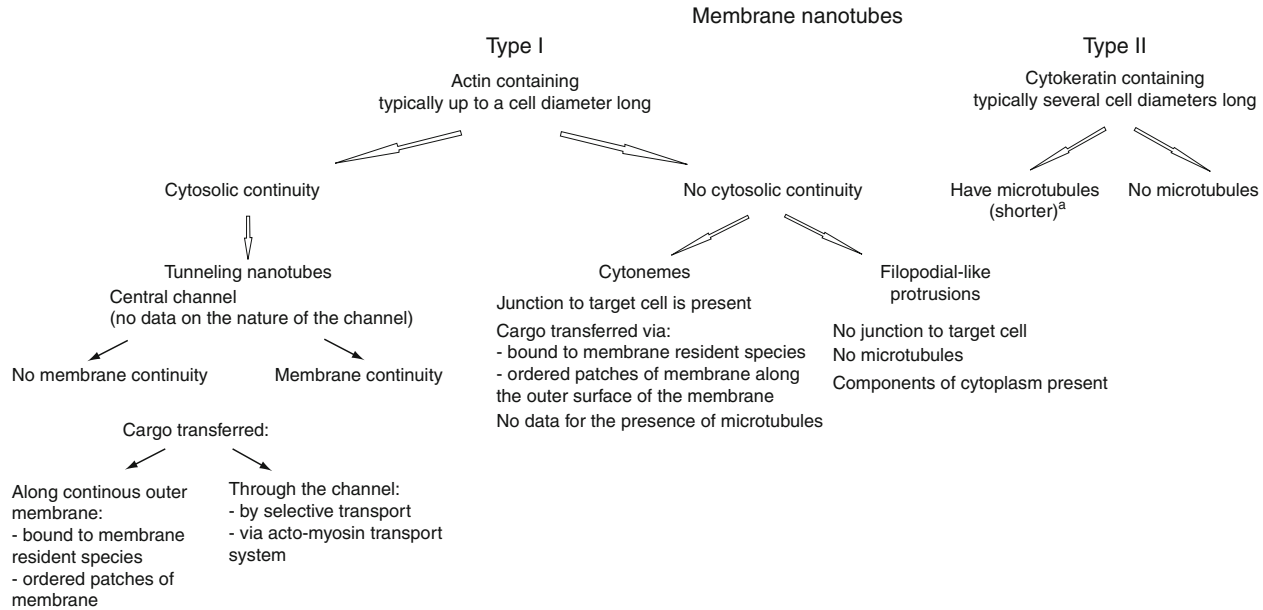


**Figure 1** *Classification and forms of membrane nanotubes.* Criteria used for classification and their main properties are briefly described. Additional remarks are described in brackets. <sup>a</sup>Unpublished observation.

The focus of this chapter will be on the properties and formation of nanotubes found in urothelial cell line T24. In our studies phase contrast, fluorescence, time-lapse and electron microscopy were employed to study structural characteristics, formation, stability and dynamics of nanotubes that bridge two neighboring urinary bladder epithelial cells T24. Theoretical models of mechanical stabilization of membrane nanotubes are suggested.

## 2. T24 CELL LINE AND MEMBRANE NANOTUBES

Cells in a permanent cell line isolated from transitional cell carcinoma of urinary bladder epithelia are heterogenous, consisting of at least two morphologically distinct types [4]. Cells grow in a disorderly manner, forming a monolayer of cells, where individual cells are lying partly over one other. Cell population consists of two main types of cells: (i) large cells with large, round, light nuclei with scarce chromatin and numerous nucleoli, abundant and slightly pyronin-positive cytoplasm (pyronin is a ribonucleic acid dye) which is rather poor in organelles, with a few mitochondria and ribosomes; (ii) elongated cells with oval, darker nuclei, with many protrusions, abundant in chromatin and several nucleoli, more strongly pyroninophilic cytoplasm with numerous mitochondria and abundant endoplasmic reticulum. Cells contain numerous vacuoles of different sizes with inclusion bodies sometimes present. Cell membrane has many protrusions, especially at the basal edges of the cells, with nanotubes connecting cells close together (Fig. 2).

Membrane nanotubes are readily formed only between closely positioned cells of a subconfluent culture, where cells have a certain degree of freedom to move around on the substratum. The most appropriate conditions for studying their properties were found to be 70–80% confluent overnight cultures grown on glass coverslips, where cells were not yet mitotic and have enough space to form membrane protrusions.

### 2.1. Types of Membrane Nanotubes, Their Structural and Functional Properties

In subconfluent culture of T24 cells two distinct types of membrane nanotubes were identified and classified with respect to their cytoskeletal content, origin, stability and consequently their proposed function (Fig. 3).

#### 2.1.1. Type I nanotubes

Type I nanotubes are shorter, usually not longer than 30  $\mu\text{m}$ , dynamic structures and contain actin filaments. Actin filaments give them their dynamic properties. The protruding type I nanotubes are formed when a

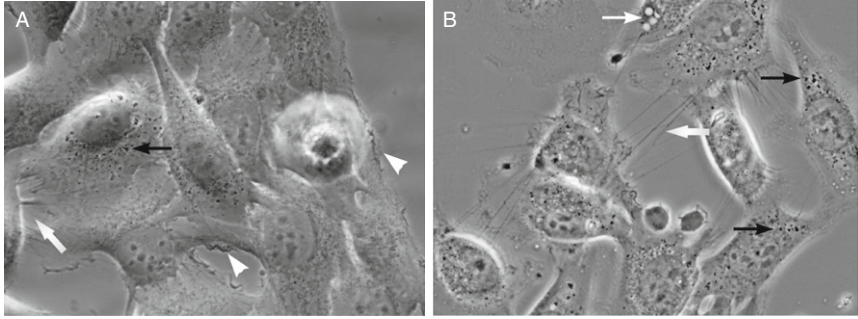


**Figure 2** *T24 cell line, grown in normal conditions.* Cells are growing partly one over other. Note that the membrane of the cells on the edge of the cell island (indicated by arrowhead in (A)) are not and firmly attached to the substratum along entire edge of the cell body, but at some places rather undulating with the cell membrane floating in the medium. Cells in the middle of the cell island are tightly connected with tubular connection forming between separating cells. Cells have numerous vacuoles (gray-white circular structures in cells, marked by white arrow in (B)) and inclusion bodies (black circular structures in cells, marked by black arrows). Individual cells are connected by membranous nanotubes (wider white arrow).

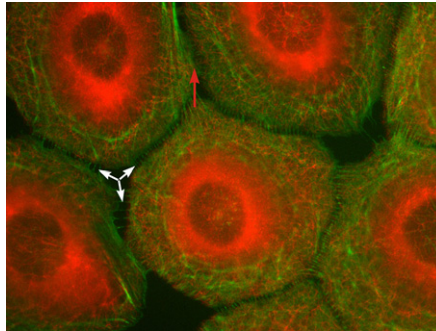


**Figure 3** *T24 cell stained for actin (gray) and cytokeratin (white) filaments.* White arrows are pointing at multiple, actin containing type I nanotubes, whereas gray arrow is pointing at longer, cytokeratin containing type II nanotube (see also Fig. 11).

cell explores its surroundings, through a thin filopodial-like tubular membrane protrusion extending from basal part of the cell body in order to make contact with another cell (Figs. 4 and 5). This type of actin-containing nanotubes can also bridge cells at distances of less than 30  $\mu\text{m}$  and is most likely derived from the adherence cell-cell contacts of cells that move apart as they appear higher on the cell body (Fig. 6). Type I nanotubes have no cytokeratin filaments (Fig. 5). Microtubules are present in some of type I nanotubes (Figs. 6B and 7). The primary function of these nanotubes seems to be intercellular communication by initiation of cell-to-cell contacts and

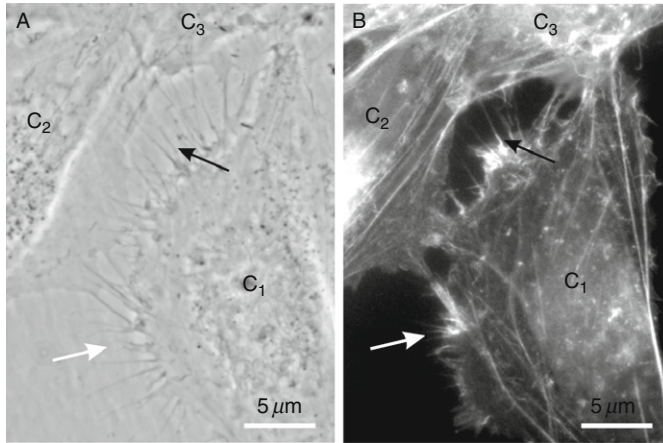


**Figure 4** Type I nanotubes. (A) is a phase contrast image of live T24 cells while (B) is a fluorescence micrograph showing actin-TRITC labeling of the same cells as in A, after 15 min of paraformaldehyde fixation. Cell C1 is approaching the cells C2 and C3 (for animation see Supplementary material I in Ref. [51]). The white arrows in (A) and (B) indicate short and dynamic membrane protrusion with which the approaching cell explores its surroundings. Black arrow in (A) points at protrusions that have already connected to the target cell. In all these multiple tubular connections actin filaments are present (arrow in B). Adapted from Veranič *et al.* [51].

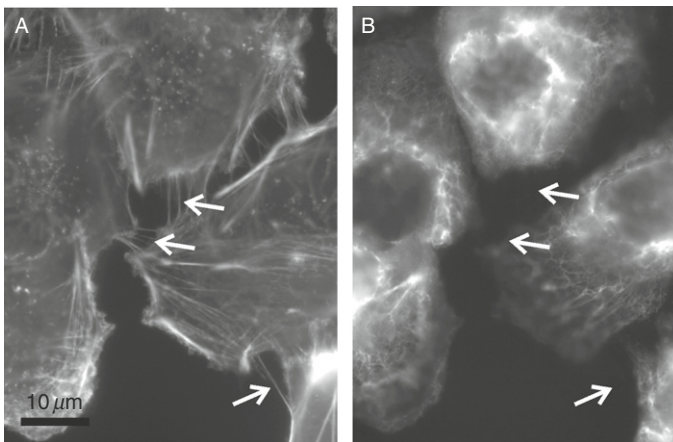


**Figure 5** T24 cells stained for actin filaments with phalloidin-FITC (A) and cytokeratin filaments with anti-cytokeratin 7 antibodies (B). Arrows (in A and B) are indicating type I containing nanotubes that bridge two cells. These structures have no cytokeratin filaments.

subsequent transport of cellular components from one cell to another once a contact has been made. Their formation and stability is discussed in Section 3.

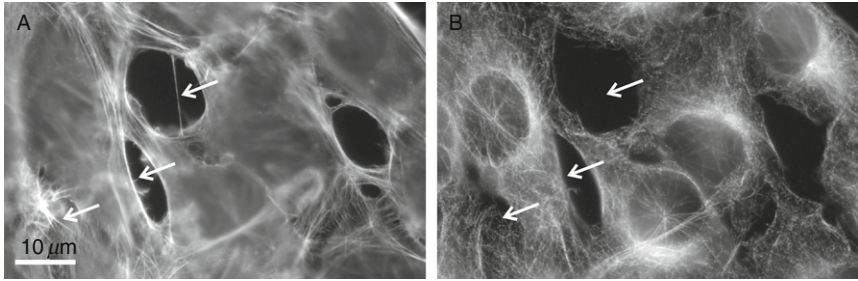


**Figure 6** T24 cells stained for actin filaments with phalloidin (A) and microtubules with anti- $\alpha$ -tubulin antibodies (B). White arrows are pointing at actin containing nanotube connecting two separated cells. Dashed arrows are pointing at dynamic acting containing nanotubes with which cell is exploring its surroundings. These structures have no microtubules. Arrows in (B) are pointing at the same parts as in (A).

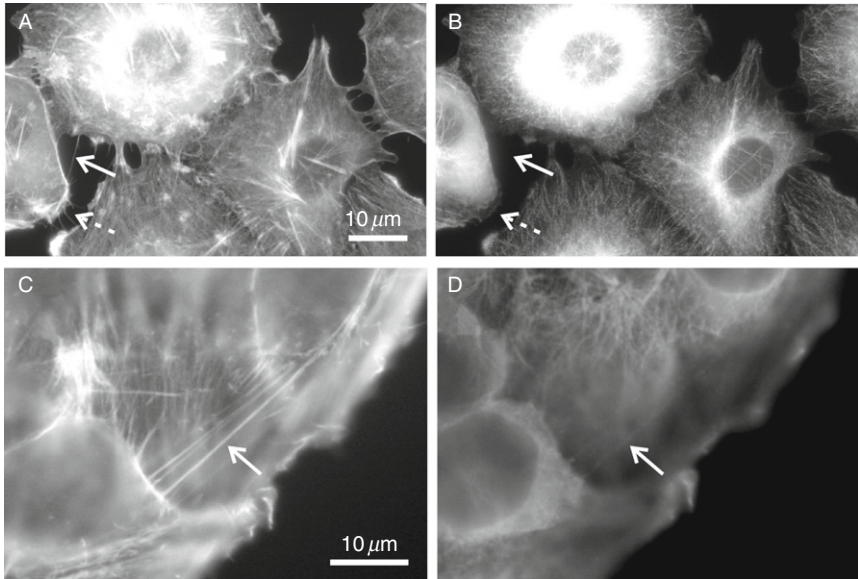


**Figure 7** T24 cells stained for actin filaments with phalloidin (A and C) and microtubules with anti- $\alpha$ -tubulin antibodies (B and D). In type I nanotubules, that search the surroundings (indicated with dashed arrows in (A) and corresponding places in (B)) or connecting two neighboring cells (indicated with arrows in (A) and corresponding places in (B)), there is no microtubules. Microtubules can be found in intercellular connections of cells that are separating (arrows in (C) and corresponding places in (D)). See also Fig. 12A and B.

The protruding type I nanotubes start growing as filopodia at the basal level of the cell surface and continue to grow until they reach the target cell (Fig. 5), where the nanotube can attach by an anchoring type of intercellular

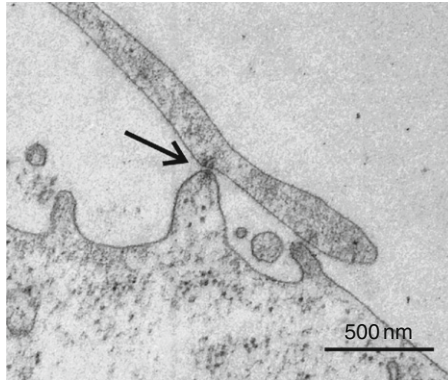


**Figure 8** A TEM micrograph showing an anchoring type of intercellular junction (arrow) connecting a nanotubule to the protrusion of a neighboring cell. Adapted from Veranič *et al.* [51].

junction [43, 51] (Fig. 8). However, it is not much known about the nature of these contacts. The connection via nanotubules may not be initiated directly by contact of the tip of the membrane nanotube with the target membrane, but may require a nanotube first to slide along target cell membrane and connect to the cell via several adherens junctions at the lateral region of nanotube (Fig. 8) before the cytosolic continuity can be established via communication junction at the nanotube tip. These adhesion contacts might also be necessary for the nanotube to stabilize the contact with the target cell when it is “searching” for appropriate docking site for the communication junction to be formed.

Proteins responsible for formation of lateral connection of the nanotubes to the target cell most likely belongs to cadherin family, since these proteins were found at both tips and tubular regions of type I nanotubular protrusions (Fig. 9).

Nanotubes in T24 cell line can mediate cytosolic continuity [16, 51] even though no exchange of membrane labels could be found between cells [51] (Fig. 10).

### 2.1.2. Type II nanotubes

In comparison to abundant type I nanotubes, type II nanotubes are quite scarce. They are much longer, up to several 100  $\mu\text{m}$  and appear to be more stable (Fig. 11). They are usually located more apically on the cell body. Type II nanotubes differ from all previously described nanotubes (which can be determined as type I nanotubes) by having no actin filaments but only cytokeratin filaments, which are probably responsible for their stability [37] and longer life span. Actin network is still present at both ends of the

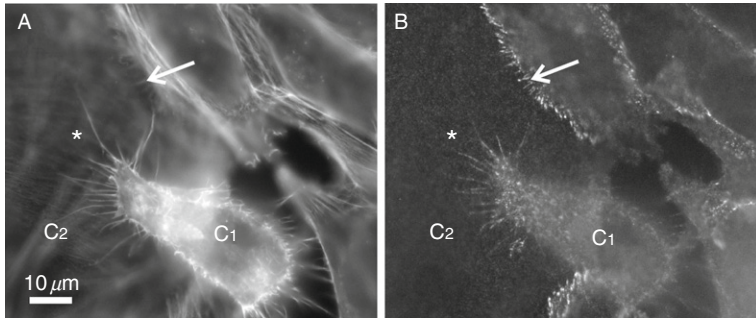


**Figure 9** T24 cells stained for actin filaments with phalloidin-FITC (A) and anti-cadherin antibodies (B). Cell C<sub>1</sub> is crawling upon cell C<sub>2</sub>. Cadherins are present at cell-cell contacts (arrow) and actin containing nanotubes (asterix), even though not at all tips of the nanotubes.

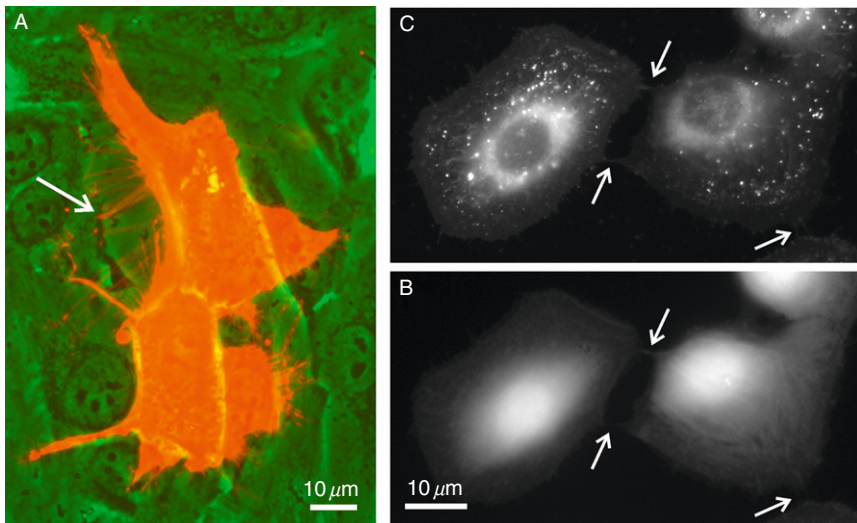


**Figure 10** (A) Urothelial cells T24 labeled with lipophilic stain DiI were cocultured with unlabelled T24 cells. The nanotubes (arrow) of stained cells (white) became protruded and attached to unstained cells (gray) in 3 h. However, even after 24 h DiI stain did not spread to the connected cells. (B) and (C) Live urothelial cells T24 colabeled with lipophilic membrane stain DiI (B) and cytoplasmic dye CMFDA (C). Nanotubes are mediating cytoplasmic connection between two neighboring cells (arrows). Adapted from Veranić *et al.* [51].

nanotube, but as the nanotube narrows actin disappears. They may be formed when two already connected cells start to move apart (Fig. 12A and B). As is the case of type I nanotubes, microtubules are present in only some of type II nanotubes, mainly those which connect separating cells (Fig. 12C).

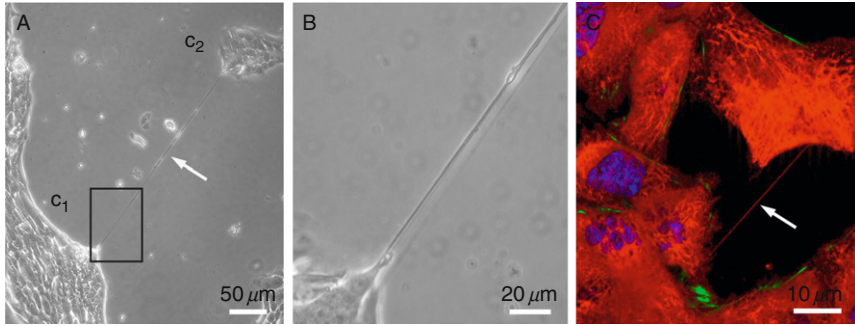


**Figure 11** In urothelial line T24 a long tubular structure connects cells of the two cell clusters  $C_1$  and  $C_2$  (A). (B) is a magnified region of the area in the black frame in (A). Such long singular tubes of type II contain thin cytokeratin filaments (arrow in (C)). In C cytokeratin 7 is labeled in white, and actin in gray. From Veranič *et al.* [51].

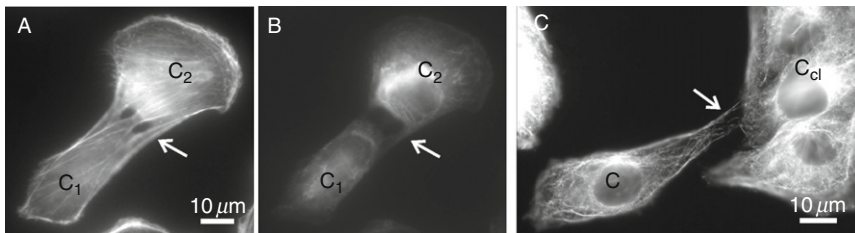


**Figure 12** (A) and (B) Two separating T24 cells ( $C_1$  and  $C_2$ ) having actin (A) and cytokeratin (B) filaments present in the forming nanotubules. (C) Cells stained for alpha-tubulin. Cell (C) is migrating away from a cluster of cells ( $C_{cl}$ ). Membranes of the two cells detach at certain sites forming tail-like protrusions between the membranes. The membranes gradually separate as the cells move apart, pulling and dividing their cytoskeletal content. Note that actin (A), cytokeratin (B) filaments, and microtubules (C) are still present in growing tubular connections (arrows in (A)–(C)). From Veranič *et al.* [51].

Type II nanotubes do not seem to be involved in transport between cells, but they rather provide a positional effect to connected cells by sensing their direction of migration and enabling reverted movement along the intercellular tether [51]. Since they are rare, their dynamics is still to be elucidated.

## 2.2. Vesicular Dilatations on Membrane Nanotubes

Many nanotubes have vesicular dilatations as an integral part of their membrane. Vesicular dilatations or gondolas, as we named them, can be seen in both types of nanotubes (Fig. 13), but they differ in size and dynamics.

Type I nanotubes frequently have smaller vesicular dilatations that can move along the tubes in both directions. These vesicular dilatations

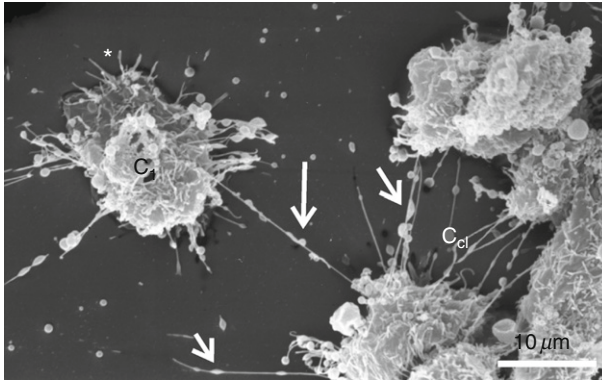


**Figure 13** A scanning electron micrograph of T24 cell line. Nanotubular structures connect adjacent cells between cell cluster ( $C_{cl}$ ) and cell  $C_1$ . Cell  $C_1$  radially extends many thin filopodial-like tubular protrusions upon the substratum in the leading part of cell (asterix). It is connected to cell cluster by a longer nanotube, located higher on the cell body. On all nanotubes vesicular dilatations are present (arrows).

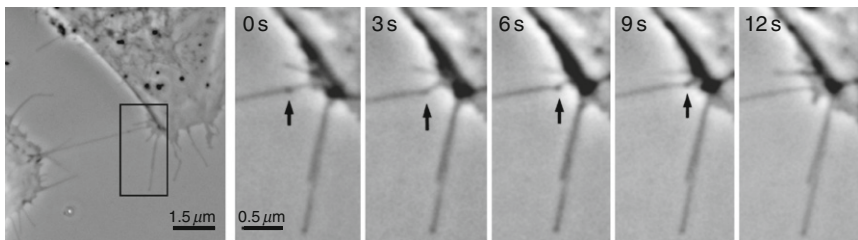


**Figure 14** Vesicular dilatation (gondola) on type I membrane nanotube (arrow). Fusion of a gondola (black arrow) with a cell body is seen after a time-lapse sequence showing directional movement of the gondola along a nanotube. The time sequence in seconds is indicated on the upper left side of each micrograph. Adapted from Veranič *et al.* [53].

(gondolas) move for 5–15  $\mu\text{m}$  in certain direction with an average speed of 40 nm/s [51]. They sometimes appear in the middle of the nanotube and travel along the nanotube until they fuse with the cell body (Fig. 14).

On the other hand, the dilatations on type II nanotubes are larger, usually placed in the middle of the nanotube and do not move along the nanotube (Fig. 15).

### 2.2.1. Possible origins of vesicular dilatations and mechanisms of their propagation along nanotubes

The observed vesicular dilatations of the nanotubes (gondolas) moving along the type I nanotubes (Fig. 16) may be formed in different ways. In some cases the formation of gondolas, corresponding to transient excited states, may be induced by a sudden tension (caused, e.g., by diverging or

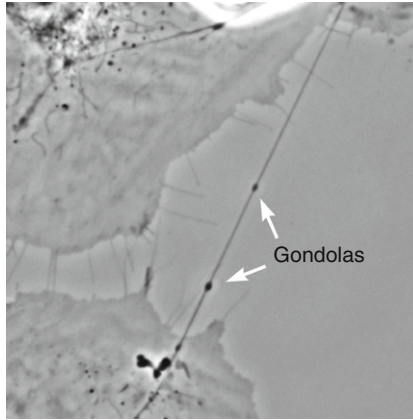


**Figure 15** Vesicular dilatations (gondolas) on type II membrane nanotubes.

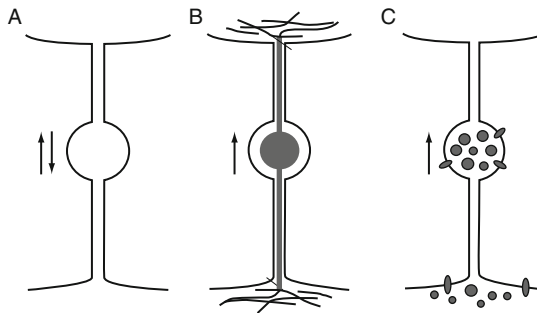


**Figure 16** Possible origins of gondola formation and its movement along a nanotube. The direction of its movement is indicated by arrows. The distention of the nanotubule (gondola) may be formed in different ways. In illustration (A) the distention is formed because of sudden tension (caused by diverging cells) in the membrane at specific sites on the nanotube, where local constituents enable and favor the formation of this structure. This kind of distention may appear anywhere along the nanotube and travels in the direction that is energetically favorable. In illustrations (B) the distention is formed because material inside the gondola is actively transported along the filaments by motor proteins ([41, 43]). The total volume of the enclosed material (an organelle or a vesicle) is larger than the inner diameter of the nanotube. Transported material (multiple small particles moving synchronously within the distention) may be enclosed within gondola or may be a part of the gondola membrane. Illustration C schematically indicates nanotubule-directed movement of the gondola, formed in the budding process.

approaching cells) in the membrane nanotubes at specific sites where the local membrane constituents of the nanotubes enable and favor the formation of such dilatations. The tension-induced dilatation of the nanotubes may appear anywhere along the nanotube and then travels as a wave along

the nanotube in the direction that is energetically favorable. The tension might be the most probable reason of gondolas that suddenly appear in the middle of the nanotube [51]. These tension-induced dilatations are as any other excited states of the membrane relaxed after a certain time. It has been reported that slight undulations are relaxed in seconds while sphere-like blobs are relaxed in minutes [2].

The vesicular dilatations of the nanotubes may also be formed because of a small organelle, vesicle or supramolecular assembly (multiple small particles moving synchronously within the distension) is being transported inside the nanotubes, if their effective diameter is larger than the inner diameter of the nanotube [15, 27, 51]. The material inside the nanotubes may be actively transported by different actomyosin-dependent mechanisms ([15, 40], reviewed by Ref. [8]). These dilatations are forming at the beginning of the nanotube of one cell as a vesicle-like structures, are transported along the nanotube and are then released into the cytoplasm of the second cell (see Fig. 17).

The observed vesicular dilatations of the nanotubes moving along the membrane nanotubes of type I show striking similarity to the dilatations of phospholipid nanotubes, which move along these nanotubes [24]. Therefore it is also possible that the initiation of gondola formation (Fig. 17A) may be based on similar physical mechanisms as those governing the formation of free membrane daughter vesicles, which are created in the processes of budding. In contrast to the latter process however, in gondolas, the connection to the parent membrane, from which they originate is not disrupted when the dilatation is detached from the parent cell (Fig. 17B). Once the gondola is formed, its movement along the nanotube (Fig. 17C) requires no additional bending energy. Nevertheless, a mechanism is still needed to provide the energy for the dilatation to travel along the nanotube. It is possible that the gondola movement is driven by the difference in chemical potentials between the molecules packed inside the gondola and the the

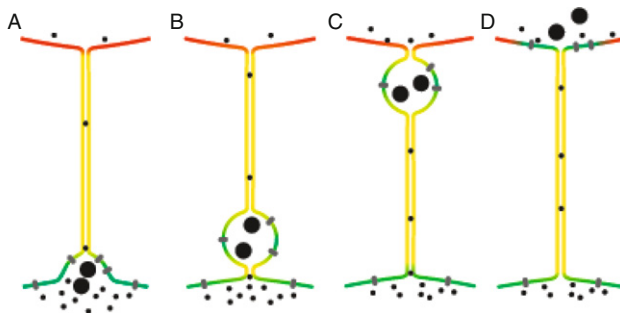


**Figure 17** Schematic illustration of nanotubule-directed transport of small vesicular dilatations (gondolas) transporting granular content and membrane particles.

molecules in the interior of the target cell, or the difference in chemical potential between the molecules composing the membrane of the gondola and the molecules in the membrane of the target cell. The final event of the transport is the fusion of the gondola with the target membrane [24]. In this process, molecules of the gondola's membrane which originate from the parent, nearly flat membrane, redistribute again in an almost flat target membrane (Fig. 17D). This may be energetically favorable and therefore also part of a driving mechanism to facilitate fusion of the gondola with the membrane. Prior to fusion of the gondola with the target cell membrane, no neck formation is needed (Fig. 17C) since the neck is already part of the nanotube connecting the gondola to the membrane of the target cell. This is contrary to the case of a free transport vesicle. It can therefore be concluded that the transport of material in dilatations (or the transport of molecules composing the membrane of dilatations) may be more efficient, since it is guided either by actomyosin transport system or passive diffusion along the nanotube, and therefore energetically advantageous over free vesicle transport.

### 3. FORMATION AND STABILITY OF TYPE I MEMBRANE NANOTUBES

Membrane nanotubes are thin, dynamic structures, but nevertheless at least transiently stable structures. We presume they are formed on (and between) specific surface regions on the cell membrane where the local environment favors their molding and stabilization (or attachment). There are several factors that influence their dynamics and stability, the major players being cytoskeleton and membrane constituents.

Although the underlying cytoskeleton greatly influences their shape, molding and mechanical stability, its primary role may not be in formation of very first steps of nanotubules but rather in strengthening the already formed membrane protrusions (nanotubular buds), to provide the core which pushes the membrane outward and on which transport of material is being conducted once the nanotube is connecting two cells. The protruding type I nanotubes in the beginning of their formation resemble the growth of filopodia (for review see Ref. [36]). Therefore it is likely that an actin cross-linker, like facsin [57], may be involved in the growth of type I membrane nanotube, by helping to organize actin filaments into parallel and nearly aligned filamentous bundles which push the membrane outward and in the stabilization of the nanotubes by increasing the stiffness of these bundles, therefore giving the tubular part of the nanotube the necessary mechanical support ([15, 40, 53, 57]). However, protrusions of this kind remain stable even after disintegration of the actin filaments with cytochalasin D (Fig. 18), that is, without the force of cytoskeleton

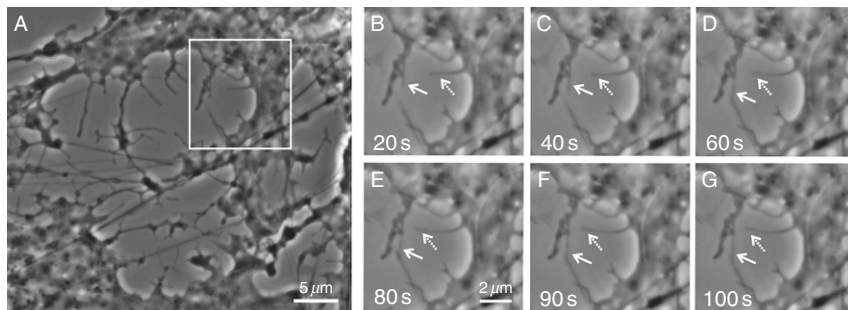


**Figure 18** T24 cells after cytochalasin D treatment (A). After incubation in cytochalasin D for 30 min, a time-lapse sequence was recorded. The flexible stability of type I membrane protrusions of T24 cells can be seen by time-lapse sequence in frames B–G (magnified region of squared area in (A)). The white arrows in these frames point to the tip of two nanotubes that passively move in the solution. Times indicated is the time passed from the beginning of the time-lapse sequence. From Veranič *et al.* [51].

elements which would push the membrane tubular protrusion outward, leaving protrusions freely diffusing in solution. These results indicate that there must also be other factors stabilizing the nanotube in addition to cytoskeleton.

Possible candidates for the stabilization of nanotubular structures are membrane nanodomains. Their membrane constituents: phospholipids, cholesterol and proteins, and their interactions with each other, may have primary role in the formation of nanotubes by forming flexible membrane nanodomains [27] (including membrane rafts) that selfaggregate at sites of the forming nanotube and thus enable the formation of nanotubular tips (see Fig. 25). They stabilize the structure in the tubular region, once the nanotube is already protruding from the membrane. This process depends on the local curvature of the membrane, which is—in turn—determined by the local composition of its constituents, their intrinsic shape and interactions with the neighboring molecules (see also Section 3, Fig. 25). In favor of this assumption is that the tips of the nanotubes tend to accumulate ganglioside GM1 (Fig. 19) as one of the characteristic components of membrane nanodomains referred to as membrane rafts. Membrane rafts are small (10–200 nm), heterogeneous, highly dynamic, sterol- and sphingolipid-enriched domains that compartmentalize cellular processes. Small rafts can sometimes be stabilized to form larger platforms through protein–protein and protein–lipid interactions [58]. The appearance of membrane rafts in vesicular protrusions at the tip of the nanotubes might also be crucial for the attachment of the nanotube to the target cell, because among proteins included in lipid raft domains N-cadherins were also found [6]. These cadherins are responsible for making intercellular connections between mesenchymal cells and are also found in urothelial T24 cells (Fig. 9).

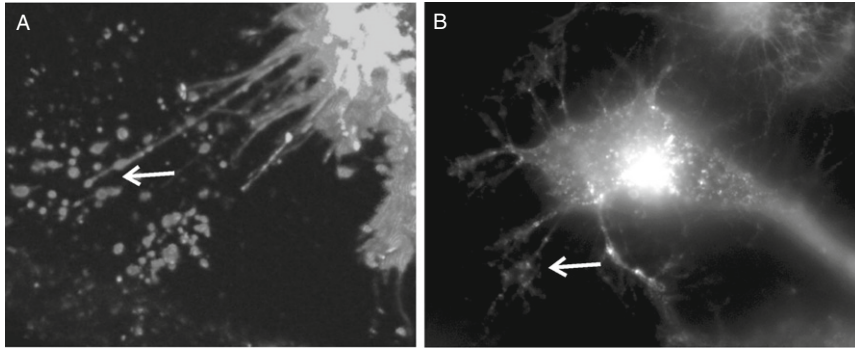


**Figure 19** Membrane rafts are present at the tips and entire length of the nanotubes as well as on cell body. Cells were stained with a membrane raft marker cholera toxin B (arrows) that binds  $G_{M1}$ , a membrane raft resident ganglioside.

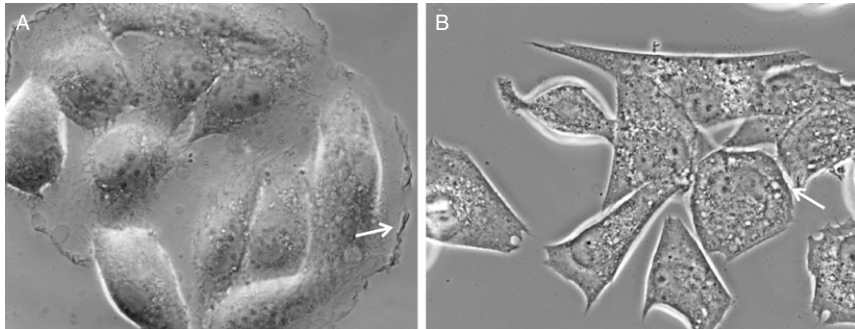


**Figure 20** Control (A) and cholesterol depleted cells (B) and their morphology. In cholesterol depleted cells the cells round and their membrane appears more rigid with no dynamically fluctuating protrusions at the cell edges like in control (arrow in (A)). Their shape is rather determined by the underlying cytoskeleton. Cells do not appear firmly attached to each other anymore, although they still preserve some connections (arrow in (B)).

Since nanodomains are thought to be important in both formation and stability of nanotubes and these nanostructures are shown to be enriched in cholesterol (Pike *et al.*, 2006) it is expected that content of cholesterol in the membrane will influence also the dynamic of nanotubes. Cholesterol decreases membrane fluidity, locally increases membrane thickness and can directly modulate the dynamics of membrane rafts-associated proteins (reviewed in Ref. [39]) as well as cell-to-cell junctions [10, 38].

Our preliminary results show that depletion of cholesterol by  $\beta$ -methyl cyclodextrin changes morphology of T24 cells as well as almost totally inhibits formation of type I membrane nanotubes, whereas the effect on type II nanotubes is not known (no experimental data) (Fig. 20).

### 3.1. On the Role of Small Anisotropic Protein–Lipid Nanodomains in Formation and Stabilization of Membrane Nanotubes

The observed stability of tubular membrane protrusions after disintegration of the actin filaments within tubular protrusions (Fig. 18) can be explained by coupling between the nonhomogeneous lateral distribution of the membrane nanodomains and the specific membrane curvatures [5, 22, 25, 45, 50]. The proposed mechanism of mechanical stabilization of tubular membrane protrusions is a part of the general mechanism of stabilization of highly curved membrane structures (spherical buds, necks, tubular protrusions) [5, 18, 23, 26, 28, 49, 50]. For example, it was suggested that due to its specific molecular shape the prominin molecules [56] may form small anisotropic protein–lipid nanodomains [26, 27] which may associate into larger two-dimensional aggregates accumulated in tubular membrane protrusions (Lubrol rafts) [23, 26, 28, 59]. Lubrol rafts, formed by clustering of prominin nanodomains, are considered to be a novel type of membrane rafts (microdomains) that are distinct from the cholesterol-sphingolipid (Triton resistant) rafts in the planar parts of the membrane [23, 28, 59].

The prevalent force of the origin of membrane protrusion is usually the force exerted by the cytoskeleton elements [3]. However, also in this case, the accumulation of anisotropic membrane nanodomains in tubular membrane protrusions may offer an additional physical mechanism for stabilization of tubular membrane protrusions [26, 32, 55]. The observed stability of thin tubular membrane protrusions without the inner supporting rod-like skeleton (Fig. 18) is in line with the assumption that prominin nanodomains (and other anisotropic membrane inclusions) have an important role in generation and stabilization of plasma membrane protrusions and TNTs; [26, 28] (Fig. 21).

In accordance with above proposed mechanism of stabilization of tubular membrane protrusions we proposed [51] that membrane nanodomains (Fig. 21) which compose the membrane of bridging nanotubes energetically prefer highly curved cylindrical geometry ( $C_1 > 0$  and  $C_2 = 0$ ) (for definition of the principal membrane curvatures  $C_1$  and  $C_2$  see Fig. 22).

In our model [12, 27] we divide the flexible membrane nanodomains in two groups. In the first are small molecular complexes composed of proteins and lipids where the proteins are often chain-like biopolymers that cross the membrane bilayer a few times (Fig. 21A) [22, 26]. Membrane nanodomains and raft elements of biological membranes usually fall into this category. The second group of flexible membrane inclusions are induced by a single rigid globular membrane protein, which can be described in the first approximation as a rigid object of a simple geometrical shape (Fig. 21B) [7, 8, 11, 12, 19, 30, 31].

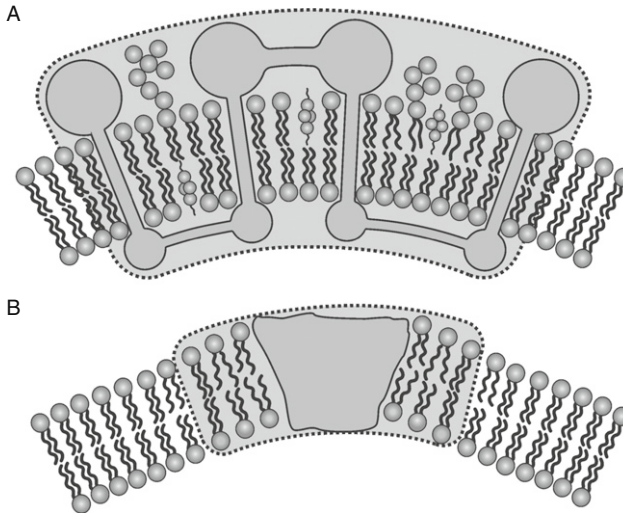


**Figure 21** Schematic illustration of membrane nanodomains (shaded area): A flexible lipid-protein membrane nanodomain containing transmembrane proteins (A) and a flexible membrane nanodomain induced by single membrane-embedded rigid (globular) protein (B) [12].

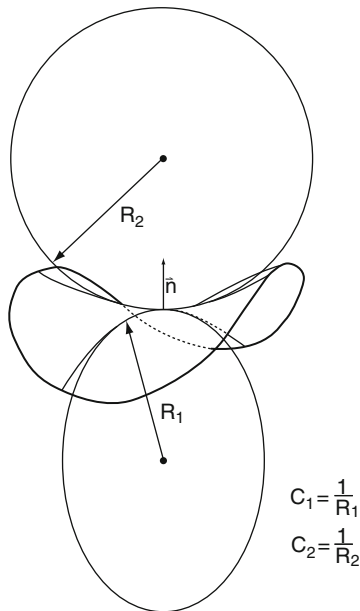


**Figure 22** Schematic presentation of the two principal membrane curvatures  $C_1$  and  $C_2$  (for the case of saddle-like membrane shape) defined in the origin of the membrane normal  $n$ . The principal curvatures  $C_1$  and  $C_2$  are inversely proportional to principal radii of curvatures  $R_1$  and  $R_2$ , respectively.

In the following we assume that membrane nanodomains (Fig. 21), as a result of their structure and local interactions energetically prefer a local geometry that is described by the two intrinsic principal curvatures ( $C_{1m}$  and  $C_{2m}$ ) [13, 31, 36]. The intrinsic principal curvatures (spontaneous curvatures) ( $C_{1m}$  and  $C_{2m}$ ) are in general different ( $C_{1m} \neq C_{2m}$ ) (Fig. 23). If they are identical ( $C_{1m} = C_{2m}$ ), the nanodomain is called isotropic. If  $C_{1m} \neq C_{2m}$  the nanodomain is called anisotropic. The location and orientation of the anisotropic nanodomain are important for its energy. An anisotropic nanodomain (Fig. 24) will therefore prefer to accumulate in the membrane region with the principal curvatures  $C_1$  and  $C_2$  close to the values of its intrinsic principal curvatures  $C_{1m}$  and  $C_{2m}$  [22, 26] and on the average also spend more time in the orientation that is energetically more favorable than in any other orientation. A coupling between the membrane shape (i.e., curvature) and the nonhomogeneous lateral distribution of membrane nanodomains has been predicted [5, 18, 22, 25, 27, 45, 50].

The elastic energy of a small anisotropic membrane nanodomain derives from the mismatch between the actual local curvature of the membrane (Fig. 22) and the intrinsic (spontaneous) curvature of the constituents (Fig. 23) which can be characterized by the mismatch tensor  $\underline{M} = \underline{R}\underline{C}_m\underline{R}^{-1} - \underline{C}$  [27]. Here the tensor  $\underline{C}$  describes the actual curvature (see Fig. 22), while the tensor  $\underline{C}_m$  describes the intrinsic curvature of the constituents:

$$\underline{C} = \begin{bmatrix} C_1 & 0 \\ 0 & C_2 \end{bmatrix}, \quad \underline{C}_m = \begin{bmatrix} C_{1m} & 0 \\ 0 & C_{2m} \end{bmatrix}, \quad (1)$$

where

$$\underline{R} = \begin{bmatrix} \cos \omega & -\sin \omega \\ \sin \omega & \cos \omega \end{bmatrix}, \quad (2)$$

is the rotation matrix. The angle  $\omega$  describes the orientation of the principal axes system of a single membrane nanodomain with respect to the local principal axes system of the membrane [28, 32]. In the respective principal

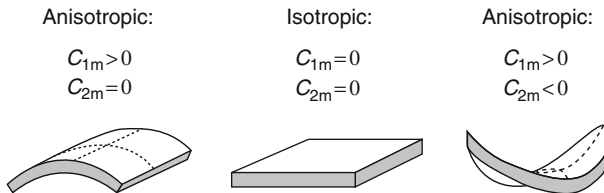


**Figure 23** Schematic representation of different intrinsic shapes of larger of membrane nanodomains described by the two intrinsic principal (spontaneous) curvatures  $C_{1m}$  and  $C_{2m}$ .

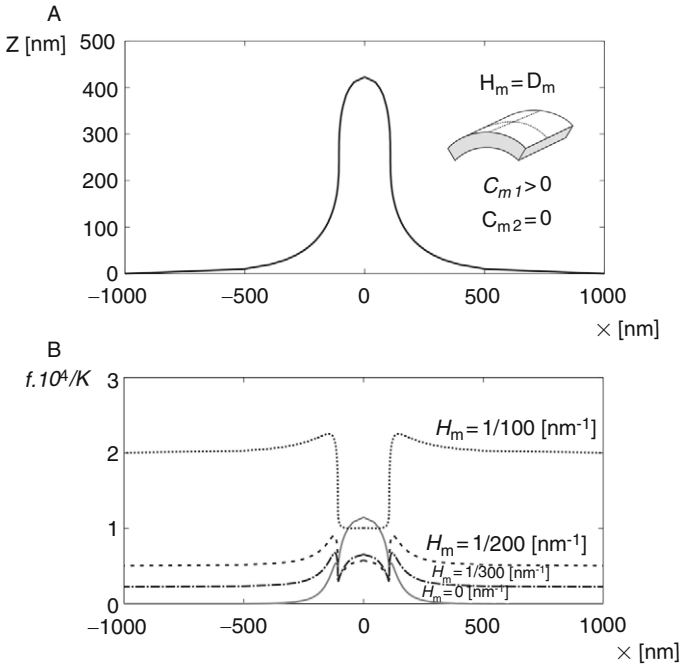


**Figure 24** Normalized free energy of single membrane nanodomain ( $f_i/K$ ) in different regions of tubular membrane protrusion and its surroundings calculated for three different shapes of membrane nanodomain characterized by  $H_m = D_m$ :  $1/100 \text{ nm}^{-1}$ ,  $1/200 \text{ nm}^{-1}$ ,  $1/300 \text{ nm}^{-1}$  and  $K = -\bar{K} = 5000kT \text{ nm}^2$  (B). The planar shape when  $H_m = D_m = 0 \text{ nm}^{-1}$  was added for comparison ((B) gray line). We assume the axis-symmetric shape of spiculum as presented in (A).

systems the matrices that represent curvature tensors  $\underline{C}$  and  $\underline{C}_m$  include only the diagonal elements (for tensor  $\underline{C}$  the principal curvatures  $C_1$  and  $C_2$  (Fig. 22) and for tensor  $\underline{C}_m$  the intrinsic principal curvatures  $C_{1m}$  and  $C_{2m}$ ).

The elastic energy of the membrane nanodomain ( $f_i$ ) should be a scalar quantity. Therefore, each term in the expansion of  $f_i$  must also be scalar, that is, invariant with respect to all transformations of the local coordinate system. In this work, the energy of nanodomain is approximated by an expansion in powers of invariants of the tensor  $\underline{M}$  up to the second order in the components of  $\underline{M}$ . The trace and the determinant of the tensor are taken as the set of invariants [27]:

$$f_i = \frac{K}{2} (\text{Tr } \underline{M})^2 + \bar{K} (\text{Det } \underline{M}), \quad (3)$$

Where  $K$  and  $\bar{K}$  are constants. Taking into account the definition of the tensor  $\underline{M}$  it follows from Eq. (3) that the elastic energy of the single membrane nanodomain can be written as [27]:

$$f_i = [(2K + \bar{K})(H - H_m)^2 - \bar{K}(D^2 - 2DD_m \cos 2\omega + D_m^2)], \quad (4)$$

where  $H = (C_1 + C_2)/2$  and  $D = |C_1 - C_2|/2$  are the mean curvature and the curvature deviator of the membrane (see also Fig. 22),  $H_m = (C_{1m} + C_{2m})/2$  is the intrinsic (spontaneous) mean curvature and  $D_m = |C_{1m} - C_{2m}|/2$  is the intrinsic (spontaneous) curvature deviator. The constants  $K$  and  $\bar{K}$  are proportional to the area of the single membrane nanodomain [12, 27]. In the case of a simple flexible membrane nanodomain composed of a rigid core (protein) and the surrounding lipids which are distorted in order to fit with the rigid core (Fig. 21), the constants  $K$  and  $\bar{K}$  were estimated using a microscopic model [12] while in the case lipid molecules they were estimated from the bending constant [34, 35]. The optimal values of the membrane mean curvature  $H$ , the curvature deviator  $D$  and the membrane constituent orientation angle  $\omega$  corresponding to the minimum of the function  $f_i$  can be calculated from the necessary and sufficient conditions for the extremum of  $f_i$  [27]:  $H = H_m$ ,  $D = D_m$ ,  $\omega = 0, \pi, 2\pi$  where  $\omega = 0$  and  $\omega = 2\pi$  describe the same orientation and where  $K > -\bar{K}/2$ ,  $\bar{K} < 0$ .

The partition function of a single anisotropic membrane nanodomain:

$$Q = \frac{1}{\omega_0} \int_0^{2\pi} \exp\left(-\frac{f_i(\omega)}{kT}\right) d\omega, \quad (5)$$

The free energy of the single anisotropic nanodomain is then obtained by considering that  $f_i = -kT \ln Q$  [27]:

$$f_i = (2K + \bar{K})(H - H_m)^2 - \bar{K}(D^2 + D_m^2) - kT \ln\left(I_0\left(\frac{2\bar{K}DD_m}{kT}\right)\right), \quad (6)$$

where  $I_0$  is the modified Bessel function. In the limit  $|2\bar{K}DD_m/kT| > 1$ , Eq. (6) becomes:

$$f_i = (2K + \bar{K})(H - H_m)^2 - \bar{K}(D - D_m)^2, \quad (7)$$

where we took into account that  $\ln I_0(x) \approx |x|$  for  $x > 1$  and  $\bar{K} < 0$ . In the limit of small  $|2\bar{K}DD_m/kT|$ , Eq. (6) transforms into:

$$f_i = \left(2K - \frac{\bar{K}^2 D_m^2}{kT}\right)(H - H_0)^2 + \left(\bar{K} + \frac{\bar{K}^2 D_m^2}{kT}\right)C_1 C_2, \quad (8)$$

$$H_0 = \frac{H_m(2K + \bar{K})}{\left(2K - \frac{\bar{K}^2 D_m^2}{kT}\right)}, \quad (9)$$

where we took into account  $\ln I_0(x) \approx x^2/4$  for  $x \ll 1$ ,  $D^2 = H^2 - C_1 C_2$  and omitted the constant term.

Figure 24 shows the influence of the anisotropy of the intrinsic shape of the membrane nanodomain (described by intrinsic mean curvature

$H_m = (C_{1m} + C_{2m})/2$  and intrinsic curvature deviator  $D_m = (C_{1m} - C_{2m})/2$  on the energy of the nanodomain  $f_i$  (Eq. (6)) in the different parts of the tubular membrane protrusions and the surrounding membrane. It can be seen in Fig. 24 that the energy of anisotropic nanodomains ( $f_i$ ) with the intrinsic shape characterized by  $H_m = D_m$  (or equivalently  $C_{1m} > 0$  and  $C_{2m} = 0$ , see Fig. 23) may be strongly decreased in the region of tubular protrusion which leads to accumulation of such nanodomains in the tubular membrane protrusion and consequently to mechanical stabilization of tubular membrane protrusions as shown elsewhere [26, 27, 32, 33, 51].

Based on the results presented in Fig. 24 and our previous theoretical consideration of the stability of tubular membrane protrusions [26, 27, 32, 33] we suggest that nanotubular membrane protrusions and membrane nanotubes are in addition to stabilization forces of cytoskeleton elements mechanically stabilized also by energetically favorable clustering of anisotropic (flexible) membrane nanodomains in nanotubes [17, 26, 27, 51] (Fig. 25).

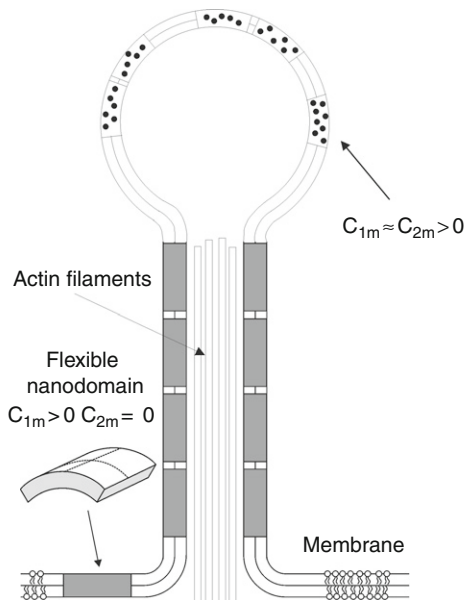


**Figure 25** Schematic illustration of stabilization of type I nanotubular membrane protrusions by accumulation of anisotropic membrane nanodomains in the tubular region. Bending deformation and rotation of the nanodomain allow the nanodomain to adapt its shape and orientation to the actual membrane curvature, which in turn is influenced by the nanodomains [23,28]. Growing actin filaments push the membrane outward. The protrusion is additionally stabilized by accumulated anisotropic nanodomains with membrane curvatures that favor anisotropic cylindrical geometry of the membrane. The cylindrical-shaped anisotropic membrane domains, once assembled in the membrane region of a nanotubular membrane protrusion, keeps the protrusion mechanically stable even if the cytoskeletal components (actin filaments) are disintegrated. Adaped from [46].

## 4. CONCLUDING REMARKS

In urothelial T24 cell line at least two different kinds of membrane nanotubes exist. These two types differ in their structural components (type I having actin cytoskeleton and type II having cytokeratins) stability, dynamics and consequently also in function. Type II nanotubes do provide cytosolic and membrane continuity between two cells, at least in the beginning, since they are presumably formed in nonmitotic separation of two cells. As for type I nanotubes cytosolic continuity can be established after an adherens and communication junctions between a protruding nanotube and acceptor cell is assembled even though their protein components have not been undoubtedly determined. Which proteins make this possible need to be further defined. Also the stability of these nanotubules is not well understood, but ongoing studies are suggesting that both cholesterol and lipid constituents that determine the local geometry of the membrane are important in this process.

## REFERENCES

- [1] B. Alberts, A. Johnson, J. Lewis, M. Raff, K. Roberts, P. Walter, *Molecular Biology of the Cell*, 4th ed., Garland Science, New York, 2002.
- [2] R. Bar-Ziv, E. Moses, Instability and “pearling” states produced in tubular membranes by competition of curvature and tension, *Phys. Rev. Lett.* 73 (1994) 1392–1395.
- [3] A.A. Boulbitch, Deflection of a cell membrane under application of local force, *Phys. Rev. E* 57 (1998) 1–5.
- [4] J. Bubeník, M. Baresová, V. Viklický, J. Jakoubková, H. Sainerová, J. Donner, Established cell line of urinary bladder carcinoma (T24) containing tumour-specific antigen, *Int. J. Cancer* 11 (1973) 765–773.
- [5] L. Cantu', M. Corti, P. Brocca, E. del Favero, Structural aspects of ganglioside-containing membranes, *Biochim. Biophys. Acta* 1788 (2009) 202–208.
- [6] M. Causeret, N. Taulet, F. Comunale, C. Favard, C. Gauthier-Rouvière, N-cadherin association with lipid rafts regulates its dynamic assembly at cell-cell junctions in C2C12 myoblasts, *Mol. Biol. Cell.* 16 (2005) 2168–2180.
- [7] N. Dan, P. Pincus, S.A. Safran, Membrane-induced interactions between inclusions, *Langmuir* 9 (1993) 2768–2771.
- [8] N. Dan, S.A. Safran, Effect of lipid characteristics on the structure of transmembrane proteins, *Biophys. J.* 75 (1998) 1410–1414.
- [9] D.M. Davies, S. Sowinski, Membrane nanotubes: dynamic long-distance connections between animal cells, *Nat. Rev. Mol. Cell Biol.* 9 (2008) 431–436.
- [10] S.A. Francis, J.M. Kelly, J. McCormack, R.A. Rogers, J. Lai, E.E. Schneeberger, R.D. Lynch, Rapid reduction of MDCK cell cholesterol by methyl-beta-cyclodextrin alters steady state transepithelial electrical resistance, *Eur. J. Cell Biol.* 78 (1999) 473–484.
- [11] M. Fošnaríč, A. Iglíč, S. May, Influence of rigid inclusions on the bending elasticity of a lipid membrane, *Phys. Rev. E* 174 (2006) 051503.

- [12] M. Fošnarič, A. Iglič, T. Slivnik, V. Kralj-Iglič, Flexible membrane inclusions and membrane inclusions induced by rigid globular proteins, *Advances in planar lipid bilayers and liposomes*, Elsevier, (2008) 143–168.
- [13] J.B. Fournier, P. Galatola, Bilayer membranes with 2-D nematic order of the surfactant polar heads, *Braz. J. Phys.* 28 (1998) 329–338.
- [14] D. Freund, N. Bauer, S. Boxberger, S. Feldmann, U. Streller, G. Ehninger, C. Werner, M. Bornhäuser, J. Oswald, D. Corbeil, Polarization of human hematopoietic progenitors during contact with multipotent mesenchymal stromal cells: effects on proliferation and clonogenicity, *Stem Cells Dev.* 15 (2006) 815–829.
- [15] H.H. Gerdes, N.V. Bukoreshtliev, J.F. Barroso, Tunneling nanotubes: a new route for the exchange of components between animal cells, *FEBS Lett.* 581 (2007) 2194–2201.
- [16] H.H. Gerdes, R.N. Carvalho, Intercellular transfer mediated by tunneling nanotubes, *Curr. Opin. Cell Biol.* 20 (2008) 470–475.
- [17] U. Gimsa, A. Iglič, S. Fiedler, M. Zwanzig, V. Kralj-Iglič, L. Jonas, J. Gimsa, Actin is not required for nanotubular protrusions of primary astrocytes grown on metal nanolawn, *Mol. Membr. Biol.* 24 (2007) 243–255.
- [18] W.T. Gózdź, Diffusion of macromolecules on lipid vesicles, *Langmuir* 24 (2008) 12458–12468.
- [19] H. Gruler, Chemoelastic effect of membranes, *Z. Naturforsch. [C]* 30 (1975) 608–614.
- [20] S. Gürke, J.F. Barroso, E. Hodneland, N.V. Bukoreshtliev, O. Schlicker, H.H. Gerdes, Tunneling nanotube (TNT)-like structures facilitate a constitutive, actomyosin-dependent exchange of endocytic organelles between normal rat kidney cells, *Exp. Cell Res.* 314 (2008) 3669–3683.
- [21] S. Gürke, J.F. Barroso, H.H. Gerdes, The art of cellular communication: tunneling nanotubes bridge the divide, *Histochem. Cell Biol.* 129 (2008) 539–550.
- [22] H. Hägerstrand, L. Mrówczyńska, U. Salzer, R. Prohaska, K. Michelsen, V. Kralj-Iglič, A. Iglič, Curvature-dependent lateral distribution of raft markers in the human erythrocyte membrane, *Mol. Membr. Biol.* 23 (2006) 277–288.
- [23] J.C. Holthius, G. van Meer, K. d’Huitema, Lipid microdomains, lipid translocation and the organization of intracellular membrane transport (review), *Mol. Membr. Biol.* 20 (2003) 231–241.
- [24] A. Iglič, H. Hägerstrand, M. Bobrowska-Hägerstrand, V. Arrigler, V. Kralj-Iglič, Possible role of phospholipid nanotubes in directed transport of membrane vesicles, *Phys. Lett.* 310 (2003) 493–497.
- [25] A. Iglič, M. Fošnarič, H. Hägerstrand, V. Kralj-Iglič, Coupling between vesicle shape and the non-homogeneous lateral distribution of membrane constituents in Golgi bodies, *FEBS Lett.* 574/1–3 (2004) 9–12.
- [26] A. Iglič, H. Hägerstrand, P. Veranič, A. Plemenitaš, V. Kralj-Iglič, Curvature induced accumulation of anisotropic membrane components and raft formation in cylindrical membrane protrusions, *J. Theor. Biol.* 240 (2006) 368–373.
- [27] A. Iglič, M. Lokar, B. Babnik, T. Slivnik, P. Veranič, H. Hägerstrand, V. Kralj-Iglič, Possible role of flexible red blood cell membrane nanodomains in the growth and stability of membrane nanotubes, *Blood Cells Mol. Dis.* 39 (2007) 14–23.
- [28] P. Janich, D. Corbeil, GM<sub>1</sub> and GM<sub>3</sub> gangliosides highlight distinct lipid microdomains with the apical domain of epithelial cells, *FEBS Lett.* 581 (2007) 1783–1787.
- [29] M. Koyanagi, R.P. Brandes, J. Haendeler, A.M. Zeiher, S. Dimmeler, Cell-to-cell 31. connection of endothelial progenitor cells with cardiac myocytes by nanotubes: A novel mechanism for cell fate changes? *Circ. Res.* 96 (2005) 1039–1041.
- [30] V. Kralj-Iglič, S. Svetina, B. Žekš, Shapes of bilayer vesicles with membrane embedded molecules, *Eur. Biophys. J.* 24 (1996) 311–321.
- [31] V. Kralj-Iglič, V. Heinrich, S. Svetina, B. Žekš, Free energy of closed membrane with anisotropic inclusions, *Eur. Phys. J. B* 10 (1999) 5–8.

- [32] V. Kralj-Iglič, A. Iglič, H. Hägerstrand, P. Peterlin, Stable tubular microexovesicles of the erythrocyte membrane induced by dimeric amphiphiles, *Phys. Rev. E* 61 (2000) 4230–4234.
- [33] V. Kralj-Iglič, H. Hägerstrand, P. Veranič, K. Jezernik, B. Babnik, D.R. Gauger, A. Iglič, Amphiphile-induced tubular budding of the bilayer membrane, *Eur. Biophys. J.* 34 (2005) 1066–1070.
- [34] V. Kralj-Iglič, B. Babnik, R.D. Gauger, S. May, A. Iglič, Quadrupolar ordering of phospholipid molecules in narrow necks of phospholipid vesicles, *J. Stat. Phys.* 125 (2006) 727–752.
- [35] T. Mareš, M. Daniel, Š. Perutkova, A. Perne, G. Dolinar, A. Iglič, M. Rappolt, V. Kralj-Iglič, Role of phospholipid asymmetry in the stability of inverted hexagonal mesoscopic phases, *J. Phys. Chem. B* 112 (2008) 16575–16584.
- [36] P.K. Mattila, P. Lappalainen, Filopodia: Molecular architecture and cellular functions, *Nat. Rev. Mol. Cell Biol.* 9 (2008) 446–454.
- [37] T.J. Mitchinson, Actin based motility on retraction fibers in mitotic PtK2 cells, *Cell Motil. Cytoskeleton* 22 (1992) 135–151.
- [38] A. Nusrat, C.A. Parkos, P. Verkade, C.S. Foley, T.W. Liang, W. Innis-Whitehouse, K.K. Eastburn, J.L. Madara, Tight junctions are membrane microdomains, *J. Cell Sci.* 113 (2000) 1771–1781.
- [39] H. Ohvo-Rekilä, B. Ramstedt, P. Leppimäki, J.P. Slotte, Cholesterol interactions with phospholipids in membranes, *Prog. Lipid Res.* 41 (2002) 66–97.
- [40] B. Önfelt, S. Nedvetzki, K. Yanagi, D.M. Davis, Cutting edge: Membrane nanotubes connect immune cells, *J. Immunol.* 173 (2004) 1511–1513.
- [41] B. Önfelt, S. Nedvetzki, R.K. Benninger, M.A. Purbhoo, S. Sowinski, A.N. Hume, M.C. Seabra, M.A. Neil, P.M. French, D.M. Davis, Structurally distinct membrane nanotubes between human macrophages support long-distance vesicular traffic or surfing of bacteria, *J. Immunol.* 177 (2006) 8476–8483.
- [42] B. Pontes, N.B. Viana, L. Campanti, M. Farina, V.M. Neto, H.M. Nussenzeig, Structure and elastic properties of tunneling nanotubes, *Eur. Biophys. J.* 37 (2008) 121–129.
- [43] A. Rustom, R. Saffrich, I. Marković, P. Walther, H.H. Gerdes, Nanotubular highways for intercellular organelle transport, *Science* 303 (2004) 1007–1010.
- [44] K. Schara, V. Janša, V. Šuštar, D. Dolinar, J.I. Pavlič, M. Lokar, V. Kralj-Iglič, P. Veranič, A. Iglič, Mechanisms for the formation of membranous nanostructures in cell-to-cell communication, *Cell. Mol. Biol. Lett.* 2009.
- [45] P. Sens, M.S. Turner, The forces that shape caveolae, In: *Lipid Rafts and Caveolae*, (C.J. Fielding, Ed.), 2006, pp. 25–44. Wiley-VCH Verlag, Weinheim.
- [46] N.M. Sherer, M.J. Lehmann, L.F. Jimenez-Soto, C. Horensavitz, M. Pypaert, W. Mothes, Retroviruses can establish filopodial bridges for efficient cell-to-cell transmission, *Nat. Cell Biol.* 9 (2007) 310–315.
- [47] N.M. Sherer, W. Mothes, Cytonemes and tunneling nanotubules in cell-cell-communication and viral pathogenesis, *Trends Cell Biol.* 18 (2008) 414–420.
- [48] S. Sowinski, C. Jolly, O. Berninghausen, M.A. Purbhoo, A. Chauveau, K. Köhler, S. Oddos, P. Eissmann, F.M. Brodsky, C. Hopkins, B. Önfelt, Q. Sattentau, D.M. Davis, Membrane nanotubes physically connect T cells over long distances presenting a novel route for HIV-1 transmission, *Nat. Cell Biol.* 10 (2008) 211–219.
- [49] C. Thiele, M.J. Hannah, F. Fahrenholz, W.B. Huttner, Cholesterol binds to synaptophysin and is required for biogenesis of synaptic vesicles, *Nat. Cell Biol.* 2 (2000) 42–49.
- [50] A. Tian, T. Baumgart, Sorting of lipids and proteins in membrane curvature gradients, *Bipophys. J.* 96 (2009) 2676–2688.

- [51] P. Veranič, M. Lokar, G.J. Schütz, J. Weghuber, S. Wieser, H. Hägerstrand, V. Kralj-Iglič, A. Iglič, Different types of cell-to-cell connections mediated by nanotubular structures, *Biophys. J.* 95 (2008) 4416–4425.
- [52] C. Vidulescu, S. Clejan, K.C. O'connor, Vesicle traffic through intercellular bridges in DU 145 human prostate cancer cells, *J. Cell. Mol. Med.* 8 (2004) 388–396.
- [53] S.C. Watkins, R.D. Salter, Functional connectivity between immune cells mediated by tunneling nanotubes, *Immunity* 23 (2005) 309–318.
- [54] D. Wüstner, Plasma membrane sterol distribution resembles the surface topography of living cells, *Mol. Biol. Cell.* 18 (2007) 211–228.
- [55] Y. Yamashita, S.M. Masum, T. Tanaka, Y. Tamba, M. Yamazaki, Shape changes of giant unilamellar vesicles of phosphatidylcholine induced by a de novo designed peptide interacting with their membrane interface, *Langmuir* 18 (2002) 9638–9641.
- [56] S. Zacchigna, H. Oh, M. Wilsch-Brauninger, E. Missol-Kolka, J. Jaszai, S. Jansen, N. Tanimoto, F. Tonagel, M. Seeliger, W.B. Huttner, D. Corbeil, M. Dewerchin, *et al.* Loss of the cholesterol-binding protein prominin-1/CD133 causes disk dysmorphogenesis and photoreceptor degeneration, *J. Neurosci.* 29 (2009) 2297–2308.
- [57] D. Vignjevic, S. Kojima, Y. Aratyn, O. Danciu, T. Svitkina, G.G. Borisy, Role of fascin in filopodial protrusion, *J. Cell Biol.* 11 (2006) 863–875.
- [58] L.J. Pike, Rafts defined: a report on the Keystone Symposium on Lipid Rafts and Cell Function, *J. Lipid Res.* 47 (2006) 1597–1598.
- [59] W.B. Huttner, J. Zimmerberg, Implications of lipid microdomains for membrane curvature, budding and fission, *Curr. Opin. Cell Biol.* 13 (2001) 478–484.